Comments on Inorganic Chemistry: A Journal of Critical Discussion of the Current Literature
Publication details, including instructions for authors and subscription information:
http://www.tandfonline.com/loi/gcic20

SINGLE CRYSTAL NEUTRON DIFFRACTION FOR THE INORGANIC CHEMIST - A PRACTICAL GUIDE

Paula M. B. Piccoli [a], Thomas F. Koetzle [a] & Arthur J. Schultz [a]
[a] Intense Pulsed Neutron Source, Argonne National Laboratory, Argonne, Illinois, 60439, USA
Version of record first published: 25 May 2007.

To cite this article: Paula M. B. Piccoli , Thomas F. Koetzle & Arthur J. Schultz (2007): SINGLE CRYSTAL NEUTRON DIFFRACTION FOR THE INORGANIC CHEMIST - A PRACTICAL GUIDE, Comments on Inorganic Chemistry: A Journal of Critical Discussion of the Current Literature, 28:1-2, 3-38

To link to this article: http://dx.doi.org/10.1080/02603590701394741

Comments on Inorganic Chemistry, 28: 3–38, 2007

ISSN: 0260-3594 print
DOI: 10.1080/02603590701394741

Taylor & Francis
Taylor & Francis Group

SINGLE CRYSTAL NEUTRON DIFFRACTION FOR THE INORGANIC CHEMIST – A PRACTICAL GUIDE

PAULA M. B. PICCOLI
THOMAS F. KOETZLE
ARTHUR J. SCHULTZ

Intense Pulsed Neutron Source, Argonne National Laboratory, Argonne, Illinois, 60439, USA

Advances and upgrades in neutron sources and instrumentation are poised to make neutron diffraction more accessible to inorganic chemists than ever before. These improvements will pave the way for single crystal investigations that currently may be difficult, for example due to small crystal size or large unit cell volume. This article aims to highlight what can presently be achieved in neutron diffraction and looks forward toward future applications of neutron scattering in inorganic chemistry.

INTRODUCTION

The impact of X-ray diffraction on the development of inorganic chemistry is undeniable. As examples from the organometallic literature we may cite Kealy and Pauson's initial report[1] on ferrocene and the resulting structure from X-ray diffraction,[2,3] along with the discovery of agostic bonds in Trofimenko's scorpionate complexes,[4–7] as seminal examples that revolutionized the way in which inorganic chemists think about structure and bonding. The automated diffractometer enabled routine structural characterization of inorganic and organometallic compounds and arguably has contributed more to the advancement of the field than any other structure characterization tool.

Address correspondence to Paula M. B. Piccoli, Intense Pulsed Neutron Source, Argonne National Laboratory, Argonne, IL 60439, USA. E-mail: ppiccoli@anl.gov

However, a major limitation of X-ray diffraction is its insensitivity to hydrogen atoms. This will hold especially when the proton is located close to a metal atom, which will dominate the scattering in the X-ray experiment. Whereas ^{1}H-NMR can provide valuable information about the chemical environment of hydrogen atoms in a compound, the particular advantage of diffraction techniques resides in its ability to determine structure at the atomic level. Neutron diffraction, with its ability to accurately locate and characterize hydrogen atoms, is ideal for providing information that cannot be gained from X-ray diffraction alone. Properties of the neutron, particularly including the fact that it scatters from the nucleus of the atom and possesses spin and a magnetic moment, make it a powerful probe for chemical structure determination and a complement to X-ray diffraction.

Fortunately, analysis of single crystal neutron diffraction data is very analogous to that of X-ray data. Widely available software packages, including SHELX[8] and GSAS,[9] can be used to refine neutron structures, thereby allowing X-ray crystallographers to conveniently perform their own analyses. As facilities at existing sources such as the ILL, SINQ, ISIS and IPNS are joined by those at more advanced neutron sources, including the Spallation Neutron Source (SNS) in the U.S.A., the KEK-JAEA Joint Spallation Neutron Source (JSNS) in Japan, the new reactor OPAL at ANSTO in Australia, and the second target station at ISIS in the U.K., which will come on-line over the next several years, opportunities for chemists to engage in single crystal neutron diffraction will increase dramatically as will our ability to handle smaller crystal sizes and larger unit cell volumes, two factors that currently limit the problems we can explore. These new facilities, with higher beam intensities and new instrumentation, will expand on the excellent science already being done at established facilities around the globe. These developments are poised to bring single crystal neutron diffraction to the doorstep of the majority of inorganic and organometallic chemists and promise greater availability than ever before.

In recent years, several comprehensive reviews on the topic of single crystal neutron diffraction in relation to chemical crystallography have been published.[10–12] It is the goal of this article to inform the greater community of inorganic chemists how neutron scattering can be utilized, now and in the future, to answer the research questions not currently addressable by conventional X-ray crystallographic techniques. We will highlight some important results from neutron diffraction of small molecules, focusing particularly on results of the last several years.

Hopefully we can address here many of the questions that new users will have when they are contemplating a single crystal neutron experiment. Neutron scattering can be useful to the chemist for a number of applications other than single crystal diffraction; for an overview we refer the reader to Roger Pynn's *Neutron Scattering: A Primer*, which provides an excellent general introduction.[13]

PRACTICAL MATTERS: THE EXPERIMENT

Properties of the Neutron

Neutrons are neutral, subatomic particles that interact with matter in a different manner than X-rays. Neutrons scatter from the atomic nuclei, whereas X-rays or electrons scatter primarily from the electrons surrounding the nuclei. As we see in Figure 1, although there is a general tendency for neutron scattering lengths to increase with atomic number, there is a quite random variation of scattering lengths between elements and, for that matter, among isotopes of the same element.

The contrast between hydrogen and deuterium, with their respective negative and positive scattering lengths, allows for good discrimination

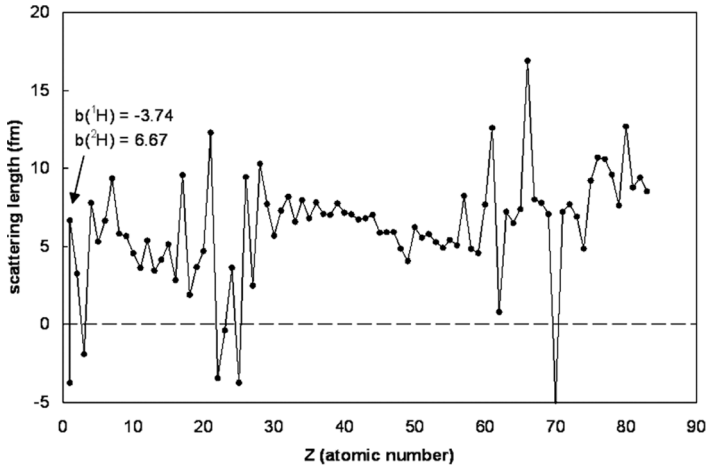

Figure 1. Neutron scattering lengths (fm) as a function of atomic number. The neutron scattering length varies quite randomly across the periodic series and, if scattering lengths are sufficiently different, neutron scattering can distinguish between neighboring elements and among isotopes of the same element. Graph constructed from the neutron scattering tables[19] and modeled after Bacon, G. E, 1975. *Neutron Diffraction*, Clarendon Press, Oxford.

between the two isotopes. The contrast can be a very useful feature, for example, when determining the percentage of deuterium in a partially deuterated complex where the fractional occupancies of H and D on the same site can be refined. This was demonstrated in the investigation of an equilibrium isotope effect in the metal hydride $H_2Os_3(CO)_{10}CH_2$.[14] Neutron diffraction data showed a preferential distribution of deuterium in the methylene ligand and hydrogen in the hydride sites, as expected on the basis of zero-point energy considerations, findings also supported by NMR. This contrasting of H and D in neutron diffraction provides especially valuable information when investigating biological structures. One ubiquitous manifestation of the negative scattering length of hydrogen is that it appears as a "hole" in neutron Fourier maps, making it extremely easy to distinguish hydrogen from other types of atoms in the structure.

Because X-rays scatter from the electron density surrounding the nucleus, heavy atoms will tend to dominate the total scattering. Furthermore, the diffuse nature of the electron distribution causes destructive interference, resulting in a decrease of the X-ray scattering factor as a function of scattering angle (this function is commonly known as the X-ray form factor). In contrast, the nucleus behaves as a point scatterer, and neutron scattering lengths accordingly do not vary with scattering angle (see Figure 2).

The neutrality and highly penetrating nature of neutron beams, along with the almost complete absence of radiation damage to the sample, combine to make neutrons an ideal probe for determining chemical structure. The properties enumerated above allow neutrons to:

- find light atoms in the presence of heavy atoms,
- distinguish between atoms of similar atomic number,
- determine magnetic structure,
- provide accurate nuclear positions and mean square atomic displacement parameters (ADP's)

In the following sections we will examine these applications in detail along with specific examples, but first we will explore some practical aspects of the single crystal neutron experiment.

Sample Size

Traditionally, the limiting factor in single crystal neutron diffraction has been sample size. Typically a crystal of not less than 1 mm^3 in volume has

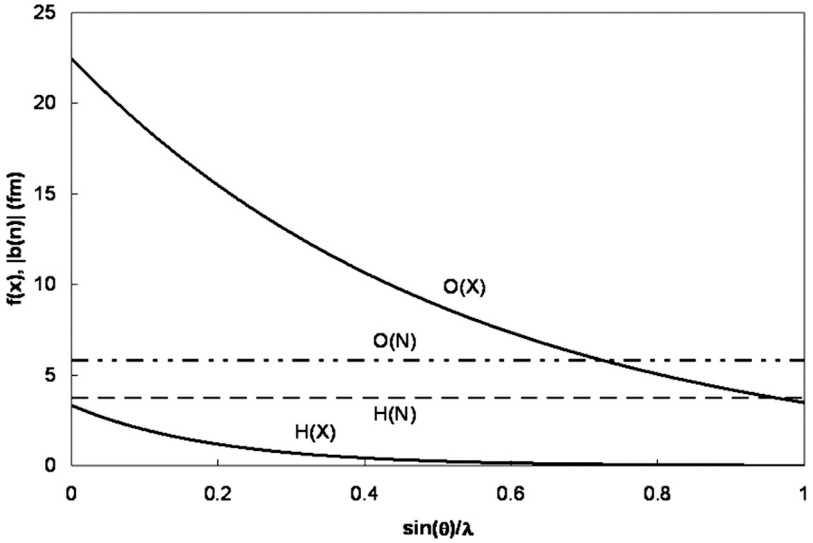

Figure 2. Scattering factors (fm) as a function of $\sin(\theta)/\lambda$ for X-rays (f(x), solid lines) compared to the corresponding neutron scattering lengths (|b(n)|, dashed lines). Destructive interference due to the scattering of X-rays from the diffuse electron cloud surrounding the atomic nucleus causes a dramatic fall-off in intensity as data are collected at higher angles. In contrast, the nucleus acts as a point scatterer, and neutron scattering lengths accordingly do not vary with scattering angle.

been essential to obtain a suitable signal for proper structure refinement, and the process of growing a crystal at least this size can be challenging, to say the least. In practice, larger crystals than the recommended minimum are often desirable to obtain an adequate signal-to-noise ratio. (See Figure 3, which depicts some representative samples used in single crystal experiments at the IPNS.) The reason for the need for large crystals is the relatively low flux available from neutron sources. An additional factor is the resolution of the instrument, which has often limited the structures that can be investigated to those having unit cell axes of approximately 25 Å in length or less. Low flux has also resulted in fairly long experiment times, although this situation has improved in recent years with the availability of higher intensity sources and the application of area detectors. The low flux can result in a low data to parameter ratio, particularly for larger structures, which in turn can make a full refinement difficult. One solution to this difficulty may be to collect X-ray diffraction data at the same temperature as the neutron data, and to refine

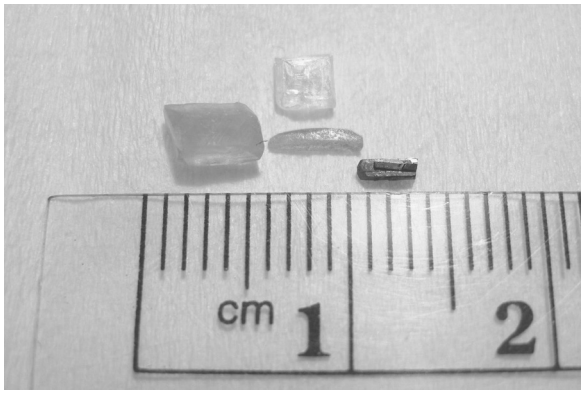

Figure 3. Some representative samples from the IPNS. Although a minimum sample size of approximately 1 mm^3 in volume is required for the typical single crystal experiment, in practice larger samples are often desirable.

both data sets jointly. In this case the heavy atoms are determined and refined primarily with the X-ray data, and hydrogen atoms are refined using the neutron data.

The advent of more intense neutron sources and new instrumentation promises to decrease data collection times as well as the minimum sample size required for the experiment. Better resolution will allow samples with larger unit cell volumes to be tackled routinely; as problems in inorganic chemistry are becoming more complex, this will be absolutely vital to addressing current research issues. Two instruments that have made major progress on this front in recent years are the LADI and VIVALDI diffractometers at the ILL in Grenoble, France. The success of LADI and VIVALDI in measuring smaller crystals and larger unit cells has led to a backlog of experiment proposals for these instruments, and clearly the demand for neutron crystallography is on the rise. To illustrate the pace of progress that has been achieved, consider that a crystal of $[N(CH_3)_4]_3[H_2Rh_{13}(CO)_{24}]$ ($1.8\,mm^3$, $a = 16.239(6)$ Å, $b = 17.887(7)$ Å, $c = 20.080(8)$ Å, $\beta = 94.62(3)^\circ$, $V = 5{,}814$ Å^3)[15] required 11 weeks of data collection time at the conventional four-circle diffractometer at the Brookhaven High Flux Beam Reactor (HFBR, since decommissioned) in 1997. By contrast, a $0.4 \times 0.4 \times 0.6\,mm^3$ ($0.096\,mm^3$) crystal of hydrogen loaded $Zn_4O(BDC)_3$(*vide infra;* cubic, $a = 25.88$ Å, $V = 17{,}334$ Å^3) required less than one day of data collection per full data set on the VIVALDI instrument in 2006.[16]

Neutron Absorption

Also of significance in neutron scattering, and often overlooked in a first time neutron experiment, is sample composition and absorption. Absorption of radiation by the sample is generally less of a problem for neutron diffraction than for X-ray diffraction. Absorption of X-rays increases with increasing atomic number, which can create a real challenge in materials containing heavy atoms. With neutrons, just as each isotope has a particular cross–section for scattering, it also has a cross–section for absorption of the neutron. A good example of the difference in absorption of X-rays versus neutrons can be easily seen in the polyoxometalate $K_7Na_9[Pt(O)(H_2O)(PW_9O_{34})_2] \cdot 21.5H_2O$, which has many heavy atoms in the structure. With linear absorption coefficient values of $\mu(X, MoK\alpha) = 257\,cm^{-1}$ and $\mu(N, \lambda = 0.7107\,\text{Å}) = 0.69\,cm^{-1}$, transmissions through a 1 mm crystal are essentially zero and 0.93, respectively. Even for a small crystal of approximately 0.3 mm, transmission is about 0.05 for X-rays. From these numbers we see that absorption is far less significant for neutrons than for X-rays.[17]

A small number of isotopes do posses a high cross–section for absorption of neutrons, and their presence can pose potential problems with data collection. For example, boron-containing composites and materials are used in neutron shielding because of boron's high absorption cross section (767 barns for natural abundance boron; 1 barn $= 10^{-24}\,cm^2$). This precludes mounting a crystal for neutron scattering in a tube containing Pyrex glass, as the neutrons will be absorbed by the boron atoms in the glass, and few neutrons will make it to the sample or the detector. Crystals that must be mounted in a capillary for the neutron experiment typically are mounted in tubes made of quartz, lead glass, or soda glass, and stabilized with plugs of quartz wool on either side of the crystal (see Figure 4). Samples that are only moderately air- or moisture–sensitive, and accordingly can withstand a short exposure time to air, are often simply coated in fluorocarbon grease prior to mounting on the diffractometer.

How does having an elemental composition containing highly absorbing components affect the neutron structure refinement? For a material containing only a few atom percent of boron in the overall structure, absorption is not a serious problem; there are many examples of neutron structures of borohydrides or other boron containing complexes in the literature. For compounds containing a high percentage of boron, for example decaborane, it may be necessary to substitute ^{11}B for natural abundance boron.[18] (An inspection of the neutron scattering tables[19]

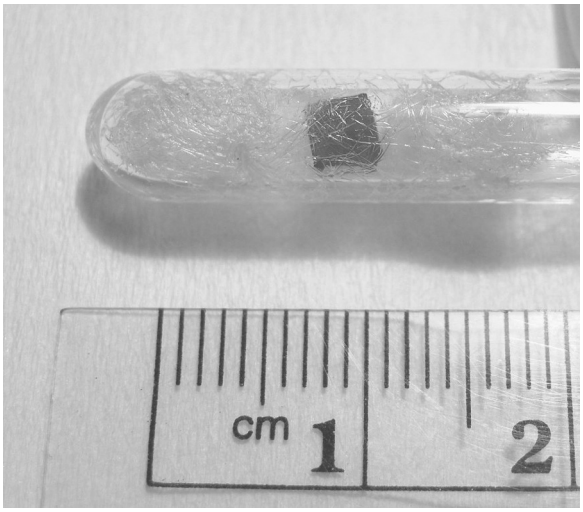

Figure 4. Air-sensitive single crystal sample sealed in a quartz tube. Plugs of quartz wool on each side of the sample help prevent it from moving in the tube during data collection.

reveals that ^{11}B has a minimal cross section for absorption, 0.055 barns.) Some members of the lanthanide series, for example gadolinium and samarium, have even higher cross–sections for absorption than boron. Without resorting to isotopic substitution neutron diffraction may not be feasible for problems featuring these elements. Of course, in the future, with smaller sample sizes absorption may not pose as large a problem.

Sample Environment

The highly penetrating nature of the neutron makes it well suited to experiments under non-ambient conditions. Neutron data for small molecules are routinely collected at very low temperatures using closed-cycle refrigerators. Experiments utilizing high-temperature furnaces, diamond anvil and gas pressure cells, and applied magnetic and electric fields are all highly feasible for neutron diffraction. Additionally, polarizers can be placed in the beam path to provide a polarized beam for analysis of magnetic structures (*vide infra)*.

Neutron Sources

The two common categories of neutron sources are steady-state reactor sources and spallation (pulsed) sources. With a reactor source, such as

the High Flux Isotope Reactor (HFIR) at Oak Ridge National Laboratory, or the High-Flux Reactor (HFR) at the ILL, the beam is generally monochromated (either by a single crystal or by choppers) to give a small range of wavelengths of radiation, similar to the normal procedure for X-ray scattering. Traditionally, a conventional four-circle diffractometer was often used in which each reflection is recorded individually using a single point neutron detector. In recent years a modified Laue technique using a band of wavelengths (adjustable to minimize peak overlap) has been developed at reactor sources and is utilized at the ILL with the LADI and VIVALDI diffractometers that were mentioned above. These instruments, with their image plate detectors, have been shown to be capable of handling smaller crystals and larger unit cells of small molecules, as well as some protein structures. The novel detector of cylindrical design allows for coverage of a large solid angle of reciprocal space and greatly reduces the time necessary for data collection. A new instrument, the KOALA diffractometer, is currently being commissioned at the ANSTO OPAL reactor and is designed after VIVALDI.

One of the first spallation or pulsed neutron source, the IPNS at Argonne, was commissioned in 1981. The LANSCE facility at Los Alamos National Laboratory and ISIS at Rutherford Appleton Laboratories in the UK followed closely behind IPNS, and most recently the SNS at Oak Ridge National Laboratory has begun production of neutrons. In addition, several spallation sources are currently under construction or in the planning stages, including the JSNS in Japan, the ISIS second target station, and the proposed European Spallation Source (ESS). Whereas reactor sources have reached a plateau with respect to practical intensity output, the spallation source design can achieve considerably higher flux (see Figure 5). In the spallation process a pulsed proton beam that has been accelerated to high energies strikes a heavy-element target. Neutrons are expelled from the target with each pulse of the proton beam, creating approximately 10–15 neutrons per proton (IPNS). The data are analyzed using the time-of-flight (TOF) technique, where neutrons are sorted by velocity v, which is related to wavelength λ by the de Broglie equation $\lambda = h/mv = (h/m)(t/L)$, where h is Planck's constant, m is the neutron mass, and t is the TOF for path length L. There is no need to monochromate the neutron beam, and so a broad spectrum of thermal neutrons can be used in data collection. With two-dimensional position sensitive detectors and a stationary crystal, this technique allows for large volumes of reciprocal space to be covered in a single

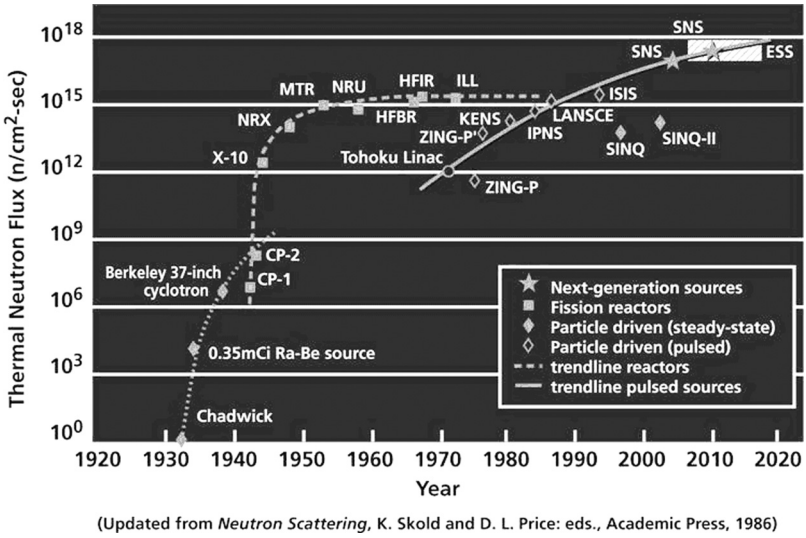

Figure 5. Neutron flux at various facilities versus year of operation.

sample orientation. Sampling this large area is especially useful for the investigation of superlattice peaks and diffuse scattering. Figure 6 shows a schematic of the SCD instrument at IPNS. The SXD instrument at ISIS works on the same principle as the SCD, but with a larger detector array that correspondingly reduces data collection time.

Data collected at any neutron source will be corrected for absorption from the sample, the incident spectrum, and detector efficiency prior to structure refinement. Extinction corrections are made during the refinement of the structure by refining an extinction parameter in a program such as GSAS or SHELX. Each facility typically has its own in-house set of programs that collect, integrate and reduce the data to structure factor amplitudes.

NEUTRONS FIND LIGHT ATOMS IN THE PRESENCE OF HEAVY ATOMS

Hydride and Hydrogen Complexes

As we have seen before, the neutron is diffracted from the nucleus of the atom and neutron scattering lengths vary quite randomly with atomic number; neutron diffraction determines nuclear positions directly and is not influenced by the electronic density, except in the special case of

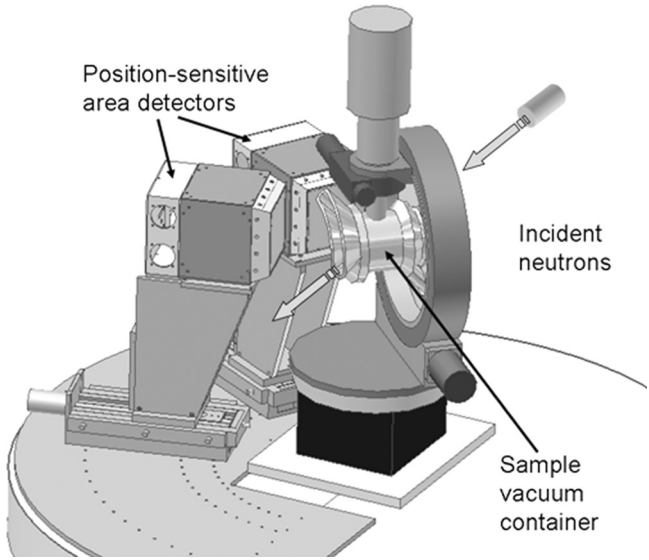

Figure 6. Diagram of the SCD instrument at IPNS. The sample is mounted in the center of the vacuum chamber and can be rotated 90° about the χ circle and 360° about φ; the ω angle is fixed at 45°. The closed-cycle refrigerator is mounted vertically on the φ axis. Two position-sensitive area detectors are centered at 75° and 120° scattering angles from the sample, and can cover a large volume of reciprocal space. The crystal is stationary during the collection of each data frame; approximately 22 settings of the diffractometer are required to cover one hemisphere of reciprocal space.

magnetic materials. These properties make neutron diffraction ideal for locating light atoms in the presence of heavy atoms. A classical application of neutron diffraction in inorganic and organometallic chemistry has concerned the location of hydrogen atoms in metal hydrides or complexes containing an agostic bond. Complexes with these features can be difficult to characterize by NMR owing to their sometimes highly fluxional nature. Numerous hydride complexes have been characterized by single crystal neutron diffraction over the years; of the 397 organometallic neutron structure entries listed as of this writing in the Cambridge Structural Database (CSD),[20] 139 of these are hydride or borohydride complexes of transition metals.

Hydride complexes of the transition metals are quite diverse, with coordination numbers of the hydride ligand in molecular complexes ranging from the 1-coordinate terminal hydrides to the 6-coordinate interstitial hydrides at the centers of octahedral clusters. The precise

location of hydride ligands bound to metal centers is not reliable with conventional X-ray diffraction methods. Bau and coworkers, leaders in the structural characterization of hydride complexes, have compiled neutron structures of hydrides through 1996 in two excellent reviews.[21,22]

The first 4-coordinate interstitial hydride was characterized only recently by the Bau group with data collected at ILL.[23] The Y_4H_8 cluster of $(Cp'')_4Y_4H_8(THF)$ [$Cp'' = C_5Me_4(SiMe_3)$] is noteworthy not only in that it contains the first example of an unusual and elusive bonding mode for a hydride ligand but also, as illustrated in Figure 7, because the cluster contains six edge bridging 2-coordinate- and one face–sharing 3-coordinate hydride ligand as well. It is thought that the presence of these additional, bridging hydrides enhances the stability of the cluster with the interstitial hydride H1 occupying the tetrahedral cavity.

The aforementioned cluster $[N(CH_3)_4]_3[H_2Rh_{13}(CO)_{24}]$ was found to possess two hydride ligands of 5-coordinate geometry (see Figure 8).[15] Each of these hydrides is sited virtually coplanar with the base of a Rh_5 square pyramid, pulled slightly out of the basal plane toward the center of the square pyramidal cavity formed by the five

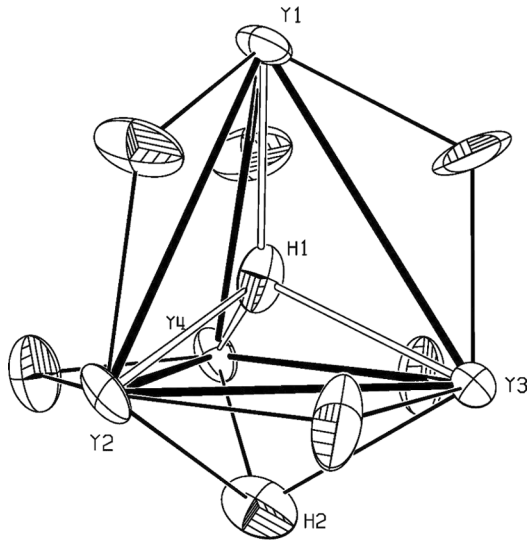

Figure 7. ORTEP plot of the Y_4H_8 core of the $[Cp''YH_2]_4(THF)$ molecule.[13] H1 is the first example of a 4-coordinate interstitial hydride. Also worthy of note is the presence of six 2-coordinate edge-bridging hydrides and the face-sharing, 3-coordinate hydride ligand H2.

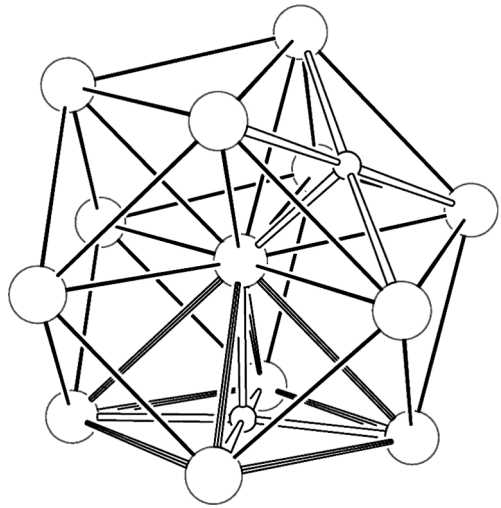

Figure 8. Plot of the $H_2Rh_{13}(CO)_{24}]^{3-}$ cluster anion, with carbonyl ligands removed for clarity. The two 5-coordinate hydride ligands are shown as small spheres, and one of the Rh_5 square pyramids is highlighted to aid the eye. The hydrides do not reside in interstitial cavities but instead are located near the surface of the polyhedron.[15]

rhodium atoms. The hydride ligands are clearly localized on two sites and are not distributed over the six available equivalent square faces of the Rh_{13} polyhedron. Rather than having hydrides located in interstitial cavities as is found in the preceding example, the structure of the $[H_2Rh_{13}(CO)_{24}]^{3-}$ cluster anion is more suggestive of hydrogen atoms chemisorbed on a Rh(100) surface.

A recent, unusual example of 6-coordinate hydrogen not involving transition metals is the interstitial hydride found at the center of the $[(t\text{-}Bu_2AlMe_2)_2Li]^-[\{Ph(2\text{-}C_5H_4N)N\}_6HLi_8]^+$ cluster, a main group complex with potential importance concerning fuel cell technology.[24] While a peak at 583 cm^{-1} in the infrared data indicated the possible presence of the hydride, ^1H NMR provided no confirmation. Single crystal neutron diffraction, in this case, was the only technique able to identify and precisely characterize the nature of the interstitial hydride (see Figure 9).

Neutron diffraction has been crucial in making the distinction between classical dihydrides and non-classical dihydrogen complexes. Characterization of dihydrogen complexes is especially important as the dihydrogen ligand represents a potential transition state in the activation of H_2 by transition metals. A recent publication from Girolami

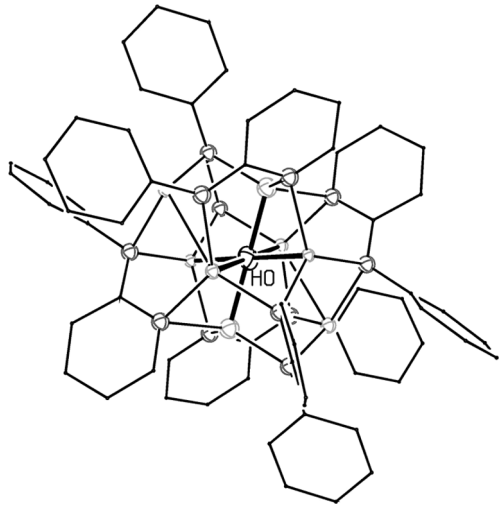

Figure 9. $[\{Ph(2\text{-}C_5H_4N)N\}_6HLi_8]+$ cation, showing the interstitial 6-coordinate hydride ligand H0 at the center of the $(Li^+)_8$ cluster. Nitrogen atoms shown in dark gray, lithium atoms in light gray.[24]

and coworkers on a series of osmium hydrides elegantly illustrates the effect of varying the sterics and electronics of the ancillary ligands.[25] As illustrated in Figure 10, changing the ligand group from PPh_3 to $AsPh_3$ results in a lengthening of the H−H bond of the dihydrogen ligand by 0.07 Å. The dihydrogen ligand is oriented parallel to the plane formed by the center of the Cp^* ligand (Ct), Os and L. Substituting PCy_3

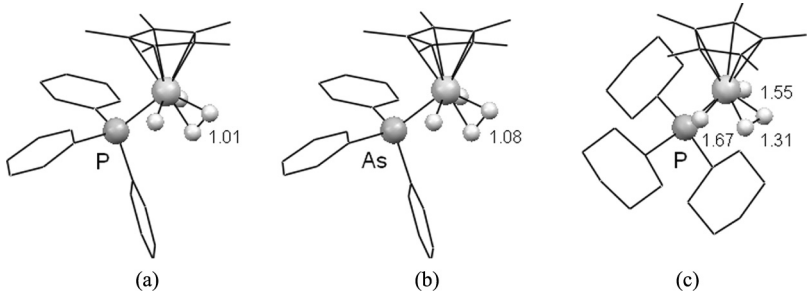

Figure 10. Neutron structures of $[Cp^*Os(H)_2(\mu\text{-}H_2)L]^+$ complexes ($L = PPh_3$, $AsPh_3$, PCy_3), showing variation in the H-H bond as a function of sterics and electronics. Bond distances in Å.[25]

for L dramatically increases the H−H distance to 1.31 Å and reorients the dihydrogen ligand to lie perpendicular to the aforementioned Ct−Os−L plane. This lengthening of the H−H bond serves as a snapshot of H−H bond activation in progress, inasmuch as H−H distances of longer than 1.50 Å are typical for classical dihydride complexes.[26]

Another important application of neutron diffraction is the location of absorption sites of hydrogen in porous, crystalline storage materials, as has been reported for Yaghi's metal-organic framework (MOF) system Zn_4O(1,4-benzenedicarboxylate)$_3$.[16,27] Inelastic neutron scattering experiments[28] have suggested that the hydrogen binding sites for a series of MOF compounds vary among compounds even though chemical makeup is quite similar, and that the nature of the organic linker in these compounds plays a significant role in how and where hydrogen is stored in these materials. In $Zn_4O(BDC)_3$, the H_2 site is clearly localized at a single framework node at temperatures between 30 and 120 K (Figure 11).

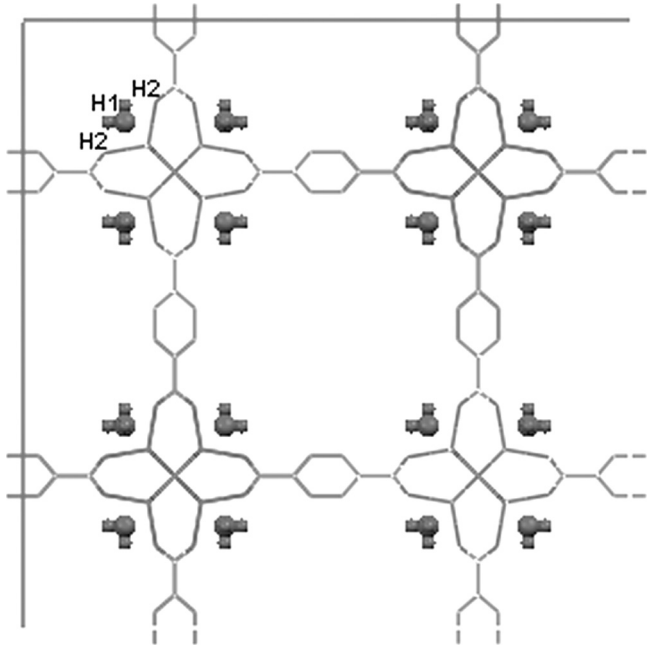

Figure 11. Plot of the unit cell for $Zn_4O(BDC)_3 \cdot 4H_2$ at 30 K. Atom H2 is disordered over three sites as atom H1 lies on a crystallographic three-fold axis. This H_2 position lies close to a framework node and is 100% occupied at 30 and 50 K. A second site, populated by H_2 at 5 K, is not shown. Hydrogen atoms on the carbon ligands have been removed for clarity.[16]

At 5 K, a second framework node is also populated at 98%. As was mentioned earlier, data collection was possible at VIVALDI, despite the very small crystal size ($0.4 \times 0.4 \times 0.6\,mm^3$), which represents a significant point in the future of single crystal neutron diffraction. As many MOF compounds form small crystals and have moderate to large unit cells, clearly this is an area for exciting growth in the very near future.

Complexes Containing Agostic Bonds

The agostic interaction,[29] where a pendant X−H bond comes into close contact with a metal center, has been a very important concept for chemists over the last twenty-five years. Molecules with this type of bond, also called transition metal σ complexes,[30] appear to be intermediates in the oxidative addition of X−H to the metal. Oxidative addition is an important step in such catalytic processes as the hydrogenation of olefins and unsaturated hydrocarbons, hydroformylation, and hydrosilation.[31] X can be any element including hydrogen (technically, in this formulation, dihydrogen species are a special class of σ complexes). The agostic bond is typically characterized by an elongation of the X−H distance, which is easily recognized by neutron diffraction. Agostic C−H−M interactions may be seen in ^{1}H NMR as well, as the chemical signal of the proton shifts to higher field ($\delta = -5$ to -15 ppm). Reduced coupling constants ($^1J_{CH} = 75$–100 Hz) can also be an indicator of an agostic interaction, although the potential fluxional nature of the interaction can obscure these signs. Vibrational frequencies at low wave numbers ($\nu_{CH} = 2700$–$2300\,cm^{-1}$) may also suggest the presence of an agostic bond. The most compelling data that we have available for such interactions are from crystal structures, and especially from neutron diffraction.[32]

The agostic interaction was first explored in the early 1970s by Trofimenko and his collaborators. NMR spectra of purported 16-electron scorpionate complexes $[H_2B(pz)_2]Mo(\eta^3\text{-}C_3H_5)(CO)_2$ and $[Et_2B(pz)_2]Mo(\eta^3\text{-}C_3H_4Ph)(CO)_2$,[4,5] indicated a shift of the methylene proton of $[Et_2B(pz)_2]Mo(\eta^3\text{-}C_3H_4Ph)(CO)_2$ into the hydridic region. The X-ray structures[7,33] revealed a close approach of the B−H or ethyl groups to the Mo center, stabilizing them as 6-coordinate, 18-electron complexes where the agostic interaction is counted as a 3-center, 2-electron bond. Recent neutron diffraction studies[34] of isostructural scorpionates $[Bp^x][Mo(CO)_2(\eta^3\text{-}C_3H_4Me)]$ (x = 3,5-Ph_2; 3,5-Me_2,4-Br;

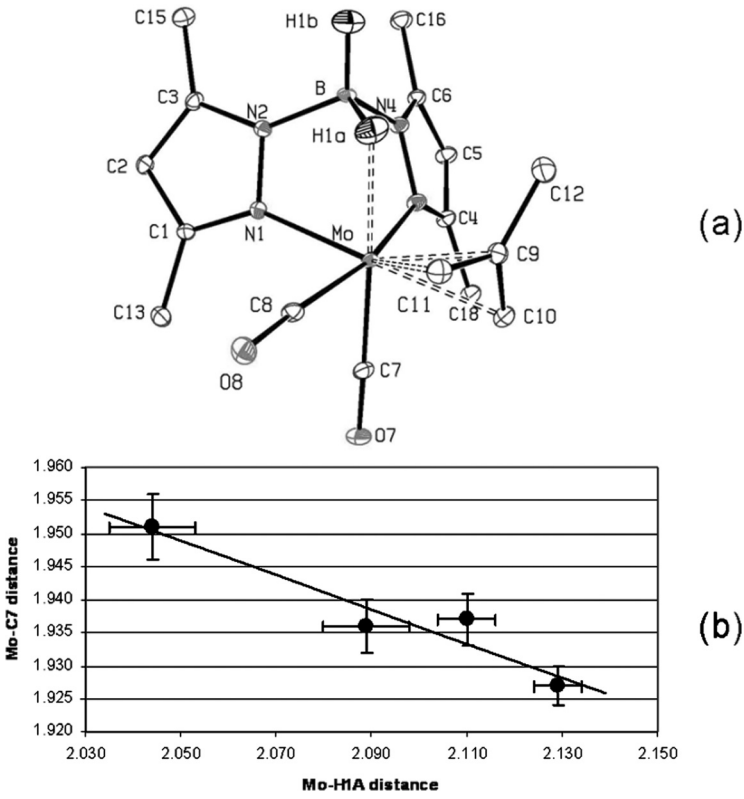

Figure 12. (a) The neutron structure of $Bp^{3,5\text{-}Me2}[Mo(CO)_2(\eta^3\text{-}C_3H_4Me)]$. (b) Plot of Mo-C7 distance versus Mo-H1A distance for a series of substituted scorpionates. As the substituents on the pyrazolylborate ligands become more electron withdrawing, the agostic Mo-H interaction becomes stronger (shorter Mo-H distance). This is reflected in the *trans*-influence, where Mo-CO distances increase with decreasing Mo-H distance.

3,4,5-Me_3; 3,5-Me_2) show, as expected, that a B−H bond is elongated by 0.05–0.08 Å, compared to an unactivated distance of 1.2 Å, when it is complexed to the metal center. A general trend is found where the strength of the agostic bond, as reflected in the Mo−H distance, is correlated with the electron withdrawing strength of the scorpionate ligand substituents. This finding is also reflected in the *trans* influence of the opposing carbonyl ligand (longer Mo−CO distances correspond to shorter Mo−H distances, see Figure 12).

The neutron structure of $TiCl_3(dmpe)Me$ (dmpe = $Me_2PCH_2CH_2PMe_2$),[35] one of the first early transition metal complexes for which an agostic M–C–H interaction was suggested,[36] shows that the internal geometry of the methyl group bound to Ti is not distorted but that the methyl group is canted towards the metal center with a Ti–C–H angle of 93.5(2)° (see Figure 13). However no elongation of the C–H bond was found. This result is consistent with the ^{1}H NMR spectrum, which finds no significant variation in the chemical shift that would indicate an agostic interaction.

An elongated C–H bond of 1.153(6) Å (versus a non-activated C–H bond distance of approximately 1.09 Å) is found for the nitrosyl complex $Cp^*W(NO)(CH_2CMe_3)_2$.[37] As with the previous example, a reduced W–C–H bond angle of 80.6(3)° is once again found. Interestingly though, in this case ^{1}H NMR spectroscopy does indicate the presence of an agostic interaction with the methylene proton signal at –1.43 ppm.[38] The complex has been described as "doubly agostic"

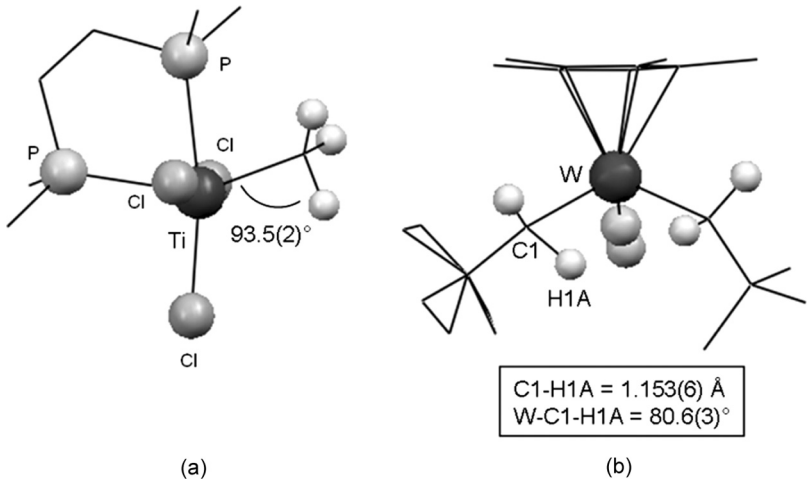

Figure 13. Neutron diffraction structures of agostic complexes: (a) $TiCl_3(dmpe)Me$[35] and (b) $Cp^*W(NO)(CH_2CMe_3)_2$.[36] In complex (a) a reduced Ti-C-H angle of 93.5(2)° is the only indication of a possible agostic interaction, as the internal geometry of the methyl group and C-H bond lengths are in the normal range. Analysis of complex (b) clearly shows an elongation of the agostic C-H bond from a typical length of 1.09 to 1.153(6)Å. The reduced W-C1-H1A angle seen in complex (a) is also seen here. Also of note for complex (b) is that the two methylene groups are inequivalent in the solid state, but in solution they both appear to have equivalent agostic interactions with the metal center. Hydrogen atoms not of interest have been omitted for clarity.

where one methylene proton on each alkyl ligand has an interaction with the metal center, although one interaction is stronger than the other. On the NMR time scale, both of these agostic methylene protons are equivalent; by contrast, they are rendered inequivalent in the solid state.

A more recent example of a "doubly agostic" complex is found in $RuCl_2[PPh_2(2,6\text{-}Me_2C_6H_3)]_2$, where the *ortho*-methyl groups on the phenyl ligands have a close approach to the metal center. As with the aforementioned tungsten example, C–H bonds are found to be somewhat elongated to 1.119(11) and 1.111(14) Å, respectively. While the ^{1}H NMR spectrum does not show the hydridic character of the agostic protons, presumably due to free rotation of the methyl groups, the ^{13}C NMR exhibits both chemical shifts and $^1J_{CH}$ coupling constants that are consistent with an agostic bond.[39] The agostic interactions stabilize what would otherwise be an unsaturated, 14-electron complex.

Just as the search for stable, multiple-bonded, transition metal-carbon complexes (alkylidene complexes) was of great interest 20–30 years ago, Mork and Tilley have recently been investigating complexes with multiple bonding between silicon and transition metals.[40] One reaction route that they have developed to prepare silylene complexes includes the activation of a Si–H bond in a $L_nM(SiHR_2)$ intermediate complex to yield a silylene hydride complex of the type $L_n(H)M{=}SiR_2$. One of these intermediate complexes, $(\eta^5\text{-}C_5Me_5)Mo(SiHEt_2)(Me_2PCH_2CH_2PMe_2)$, was isolated, and its neutron structure provides a snapshot of the intermediate in the oxidative addition of a Si–H bond to a metal. The structure, shown in Figure 14, is that of a three-legged piano stool with one leg consisting of a Si–H σ bond complex with the molybdenum. The molecule formally contains a 16-electron system in the absence of the Si–H σ bond interaction with the metal center. As observed previously, formation of a 3-center, 2-electron, σ-complex bond achieves a stable 18-electron configuration. The Mo–Si bond length of 2.34(1) Å is longer than the values of 2.219(2) and 2.288(2) Å in complexes with multiple Mo–Si bonds.[41] The Si–H bond length, 1.68(1) Å, is indicative of a significant degree of activation in comparison to a normal Si–H bond length of 1.48 Å in tetrahedral silanes. The third leg of the piano stool points in between the Si and H(1) atoms, as exhibited by the Si–Mo–P(1) and Si–Mo–P(2) angles of 87.1(3)° and 101.9(4)°. The plane of the Si atom and the two α-C atoms of the ethyl groups is nearly co-planar with the Mo atom and nearly perpendicular to the plane of the Cp^* ligand. This orientation may be indicative of π-bonding with the metal.

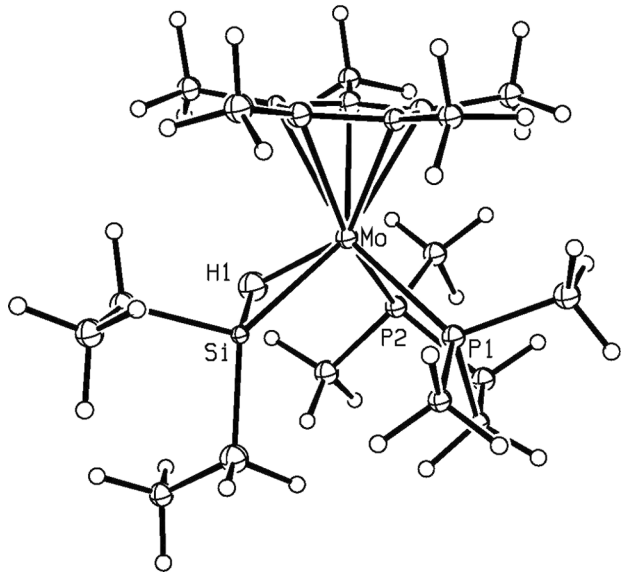

Figure 14. Neutron structure of (η^5-C_5Me_5)Mo($SiHEt_2$)($Me_2PCH_2CH_2PMe_2$) illustrating the Si-H-Mo agostic-type interaction. Except for H1, the hydrogen atoms have been displayed as small spheres for clarity, although they were refined with isotropic displacement parameters.[40]

While only a few agostic systems have been studied by neutron diffraction, it is clear that spectroscopic techniques are not always adequate to address agostic bonding issues. Neutron diffraction remains the most powerful method to locate an agostic hydrogen atom.[42]

Absence of a Hydrogen Atom

Neutron diffraction is useful in situations where it may be important to confirm the absence of a proton. This type of problem arose recently in the case of late transition metal oxo (LTMO) complexes. LTMO species, the existence of which has long been doubted, have recently been synthesized by the Hill group.[17] In conjunction with other characterization techniques, neutron diffraction was an essential tool in helping to preclude better precedented terminal hydroxyl complexes of Pt and Au (see Figure 15) LTMO polyoxometalates (POMs). Lattice water molecules were clearly visible in the neutron difference Fourier maps, and the refinement of some of these water molecules was stable; this

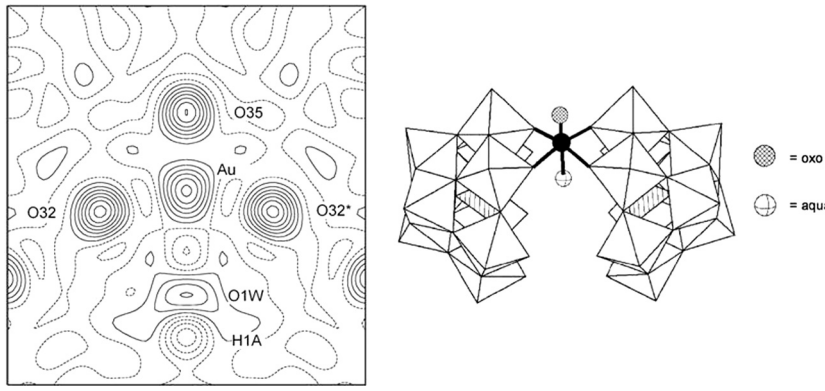

Figure 15. FOBS map (left) of the Au-oxo-POM-aqua plane in $K_{15}H_2[Au(O)(OH_2)P_2W_{18}O_{68}] \cdot 25H_2O$ (anion shown at right). Solid contours indicate positive neutron scattering density and broken contours represent negative scattering density (indicative of hydrogen atoms). Negative scattering density that models as hydrogen atoms is seen close to the disordered aqua ligand OW1, but no such density is seen in the vicinity of the O35 oxo ligand. This map is typical for both the Pt and Au terminal oxo complexes. Figure at right reprinted from reference 17.

showed that hydrogen atoms located from the neutron diffraction experiment were both real and refineable. No features in the vicinity of the terminal oxo ligand were consistent with hydrogen bound to the oxygen atom, and so the results are consistent with a terminal oxo ligand. Molecular orbital calculations on model LTMO complexes indicate that the POM ligands act as an electron sink, reducing destabilizing electron-pair repulsions.

Hydrogen Bonding

Hydrogen bonding has long been a subject explored in great detail by neutron scattering in work dating back, for example, to the pioneering studies of Peterson and Levy on the structure of ice.[43] Hydrogen bonding in small molecule organic systems[44] and in macromolecules[45] has attracted much attention. The paramount importance of the hydrogen bond in biological systems has recently motivated the development of new and improved instrumentation for neutron protein crystallography.[46–48] For the inorganic chemist, particularly with compounds synthesized hydrothermally or solvothermally, or supramolecular structures utilizing hydrogen bonding as their method of self-assembly and

organization, neutron diffraction would prove invaluable for complete characterization of the system. Since such compounds usually possess a large unit cell volume or grow as small crystals, much science in this rapidly growing field has yet to benefit from single crystal neutron diffraction.

Characterization of the hydronium ion $(H_5O_2)^+$ and aquo complexes of metals is readily achievable with neutron diffraction, which can provide structural information not accessible with X-ray methods alone. Taking into consideration the location of hydrogen atoms, the true point group symmetry for an aquo metal complex can be resolved only by locating the water hydrogens. This will also indicate whether the water ligands are pyramidal or planar with respect to the $M-OH_2$ bond. In the case of $[V(H_2O)_6][H_5O_2](CF_3SO_3)_4$, for example, the VO_6 framework has O_h symmetry, which is lowered to D_{3d} when considering the geometry of the essentially planar metal-bound water molecules.[49] The neutron data thus support the lowering of the degenerate ground state of O_h or T_h symmetry for the d^2 metal center as required by the Jahn–Teller theorem. The hydronium ion in $[V(H_2O)_6][H_5O_2]C(F_3SO_3)$ is characterized by pyramidal waters with a strong, centered hydrogen bond where the proton lies on a crystallographic center of inversion.

Neutron diffraction has been used to characterize the role of the extended hydrogen bonding network in the cooperative Jahn–Teller switch in ammonium copper sulfate Tutton salts. In 1984, it was reported from neutron powder diffraction data that the Jahn–Teller elongation of two *trans* $Cu-O$ bonds in the perdeuterated salt, $(ND_4)_2[Cu(D_2O)_6](SO_4)_2$, is orthogonal to the elongated bonds in the fully hydrogenated salt.[50] A subsequent single crystal neutron investigation of $(ND_4)_2[Cu(D_2O)_6](SO_4)_2$ under applied pressure[51] demonstrated that the switch is reversible (Figure 16) and led to several powder diffraction studies exploring the pressure-temperature phase diagram.[52] Because the scattering lengths for hydrogen (−3.74 fm) and deuterium (6.67 fm) differ by sign and magnitude, it is possible to obtain the H/D ratio and distribution by refinement of the scattering from each hydrogen site. Thus, from single crystal data, it was determined that a 42% deuterated crystal exhibited no indication of a phase transition, even though the structure had been shown to switch at 50% deuteration from EPR measurements.[53] All of these studies highlight the ability of neutron diffraction to precisely locate and refine hydrogen atoms with anisotropic ADP's, to determine H/D ratios, and to easily utilize pressure cells due to the high penetrating ability of neutrons.

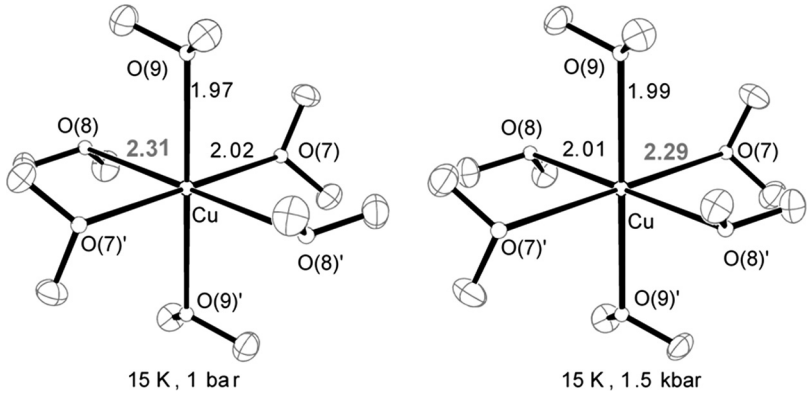

Figure 16. Results from a single crystal neutron diffraction study of $(ND_4)_2[Cu(D_2O)_6](SO_4)_2$ at ambient pressure (left) and under an applied pressure of 1.5 kbar (right). Note the changes in the Cu-O bond distances.[51]

The hydrogen bond, or hydrogen bridge,[54] is an immensely useful non-covalent interaction in crystal engineering and supramolecular chemistry,[55] and neutron diffraction is uniquely suited to probe how these relatively weak interactions influence the overall structure of molecules in the solid state. D−H···A systems can involve anything from the classic example where the acceptor A is oxygen or nitrogen, to systems where A is an aromatic π system or a halogen.[56] For example, the close intramolecular C−H···X interactions of the terminal halide ligands in linear hydride complexes $[(dippm)_2Ni_2X_2](\mu\text{-H})$ (dippm = 1,2-bis(diisopropylphosphino)-methane; X = Br, Cl)[57,58] grip the halide into a "locked" position, suggesting that these kinds of interactions may directly influence the geometry of the bridging hydride. The M−H−M angles of 177.9(10)° and 177.5(11)° are far greater than those for all other M−H−M bridging systems having a *bent* geometry (angles typically less than 160°).[22] Related complexes $[(dcpm)_2Ni_2X_2](\mu\text{-H})$ (dcpm = 1,2-bis(dicyclohexylphosphino)methane; X = Br, Cl)[58,59] do not possess the same close approaches of C−H to X due to the steric bulk of the ligand, and the geometry of the bridging hydride appears to be bent. While the neutron structures of these bent $[(dcpm)_2Ni_2X_2](\mu\text{-H})$ complexes have yet to be determined, the published result provides a fine example of how neutron crystallography can probe the effect of steric and electronic factors for a series of related compounds (see Figure 17).

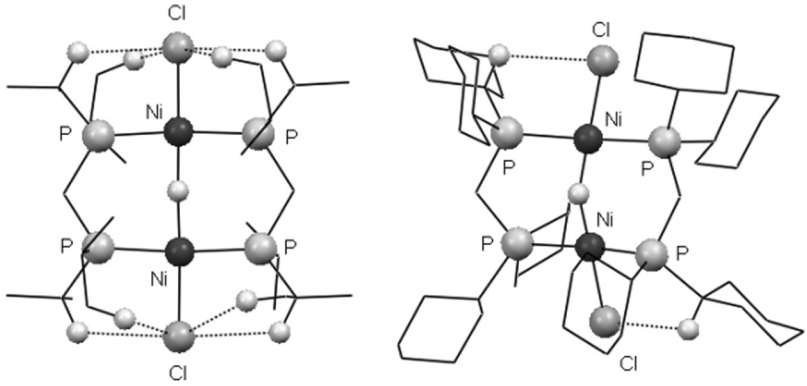

Figure 17. Comparison of the unsupported bridging hydride complexes $[(dippm)_2Ni_2Cl_2](\mu\text{-}H)$ (neutron structure, left) and $[(dcpm)_2Ni_2Cl_2](\mu\text{-}H)$ (X-ray structure, right). C-H···Cl contacts shorter than the sum of the van der Waals radii (2.95 Å) are shown as dashed lines. The sterics of the phosphine ligand are suggested to be the influencing factor on the geometry of the bridging hydride. In the linear example, the close approach of the isopropyl groups "locks" the chlorides into place, resulting in a linear hydride complex. Hydrogen atoms not involved in the hydrogen bridges have been omitted for clarity.[57–59]

NEUTRONS CAN DISTINGUISH BETWEEN ATOMS OF SIMILAR ATOMIC NUMBER

While location of atoms heavier than hydrogen is generally not a problem for the X-ray diffraction experiment, it is extremely difficult for X-rays to distinguish between two atoms of similar atomic number that reside in the same structure or occupy the same crystallographic site. The difference between X-ray scattering factors for adjacent atoms in the periodic table is often not sufficient to make this distinction. The largely random variation in neutron scattering lengths over the periodic series or between isotopes of the same element (see Figure 1) makes neutron diffraction well suited to answer questions regarding chemical identity or fractional occupancy of similar atoms, provided that the difference in scattering length between the atoms or isotopes in question is sufficiently large.

The quaternary aluminum silicide $Pr_8Ru_{12}Al_{49}Si_9(Al_xSi_{12-x})$, grown from an aluminum melt, was studied by neutron diffraction to determine not only which sites were occupied by Al and Si, but also the degree of fractional occupancy over one of the sites. Neutron results determine the

value of x to be approximately 4, in agreement with the energy dispersive spectroscopy (EDS) measurements.[60] The Kanatzidis group conducted a similar study on a crystal of $Tb_4FeGa_{12-x}Ge_x$ in which it was found that Ga partially occupies the Ge *12e* site in the structure.[61] The neutron diffraction result in this study was also consistent with EDS analysis. Neutron diffraction on the solid solution clathrate $Ba_8Al_{14}Si_{31}$ revealed that Al is substituted over all of the framework sites in the crystal, a finding also supported by ^{27}Al MAS NMR.[62]

During the analysis of neutron diffraction data from a single crystal of $(CO)_5Re(\mu\text{-}H)Mn(CO)_4Mn(CO)_5$ (Figure 18), the isotropic displacement parameters of the Re and Mn(2) atoms refined to unusual values.[63] Subsequent refinement of the scattering lengths of these atoms revealed that the terminal Mn(2) site was partially occupied by approximately 9.2% Re due to a co-crystallization of the isomorphous $(CO)_5Re(\mu\text{-}H)Mn(CO)_4Re(CO)_5$. The scattering length of the Re site refined to more than that of its reported value, but was consistent with

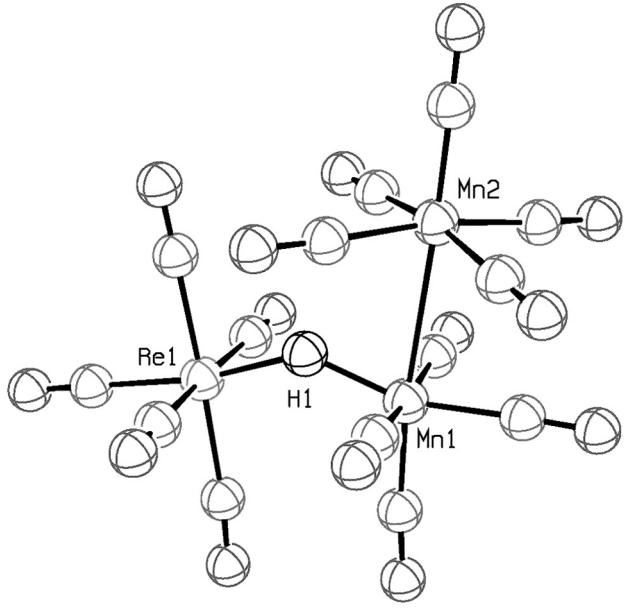

Figure 18. Neutron diffraction structure of $(CO)_5Re(\mu\text{-}H)Mn(CO)_4Mn(CO)_5$. The Mn2 site was found to be 9.2% occupied by Re due to a co-crystallization of the isomorphous $(CO)_5Re(\mu\text{-}H)Mn(CO)_4Re(CO)_5$.[63]

the scattering length obtained from the refinement of $[ReH_7\{P(p\text{-tolyl})_3\}_2]$.[64] Once the occupancy of the Mn(2) site was adjusted to reflect the site substitution of Mn by Re, and the scattering length for Re was refined and corrected, anisotropic displacement parameters had reasonable values for all metal atoms. The findings from the neutron diffraction study prompted a re-evaluation of the NMR data and helped to also postulate a mechanism for metal-metal exchange to form the co-crystal. While this is not an example of diffraction concerning near neighbors, in this case the contrast between the negative scattering length of Mn (−3.73 fm) and the highly positive scattering length of Re (9.2 fm) proved to be crucial to recognizing the site substitution, which had been missed in the X-ray structure.[65]

NEUTRONS DETERMINE MAGNETIC STRUCTURE

One of the interesting features of the neutron is that it has a magnetic moment, meaning that it behaves as a very small bar magnet. When the neutron encounters an atom with unpaired spin in an ordered magnetic material, such as we find in ferromagnets, antiferromagnets, and in paramagnetic materials when placed in a strong orienting field, the magnetic interaction gives rise to magnetic scattering, which may or may not coincide with the ordinary nuclear Bragg scattering. An important difference between magnetic and nuclear scattering is that the magnetic component is proportional to the sine of the angle between the diffraction vector and the spin. For magnetic materials, the neutron scattering is thus dependent on the direction and spatial distribution of magnetization.[13]

With an unpolarized beam the neutrons arrive at the sample with their spins in random orientations. This type of beam can still be very useful in characterizing ferro- and antiferromagnets. The use of a polarizer enables the separation of neutrons that are "spin-up" and "spin-down" for use in more complex magnetic scattering experiments. A magnetic guide field between the polarizer and sample ensures that neutrons of one spin type arrive at the sample without reverting to the random orientation of an unpolarized beam. For paramagnetic materials the spin density can be determined by aligning the spin of the sample in a magnetic field, usually at low temperature, and measuring the Bragg scattering containing both nuclear and magnetic contributions. The magnetic structure factors are Fourier components of the spin density, and can be

extracted from measurements with neutrons that are both in the "spin-up" and "spin-down" orientations. The spin density can then be constructed, for example by means of a multipolar refinement of the spin density around the nuclear positions. This method was used successfully in 1994 by Zheludev et al. in the investigation of $[Bu_4]^+[TCNE]^{\cdot -}$ (TCNE = tetracyanoethylene) at 1.8 K in an applied field of 4.65 T.[66] After determination of the nuclear structure with both X-rays and neutrons, 211 independent Bragg reflections were collected with neutrons in both orientations. The crystal was mounted in two separate orientations to maximize the number of reflections scattered from the plane of the molecule; free rotation of the sample for full coverage of reciprocal space is not yet achievable for this type of experiment. The results after multipolar refinement of the spin density on the radical anion are shown in Figure 19, in which the electronic spin density is localized on the sp^2-carbon atoms and also on the nitrogen atoms.

The rare earth complex $Y(HBPz_3)_2(DTBSQ)$, ($HBPz_3$ = hydrotrispyrazolylborate and DTBSQ = di-*tert*-butylsemiquinonate) was investigated using polarized neutrons to determine the spin density of the anion in this paramagnetic complex.[67] The $S = 1/2$ ground state is

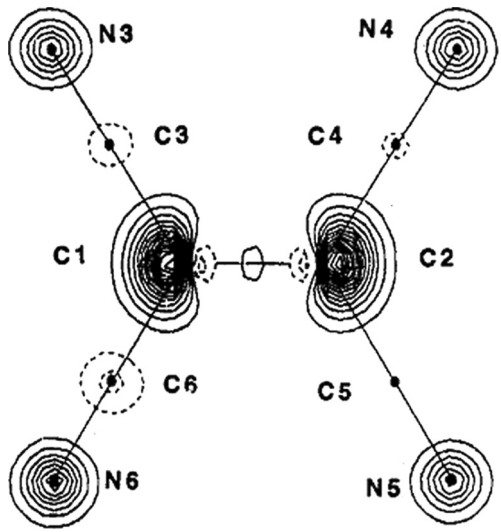

Figure 19. Magnetic spin density reconstructed by multipole model refinement, projected onto the $[TCNE]^{\bullet -}$ molecular plane. Reprinted with permission from Zheludev, A., et al. 1994. *J. Am. Chem. Soc.* 116:7243–7249. Copyright 1994, American Chemical Society.[66]

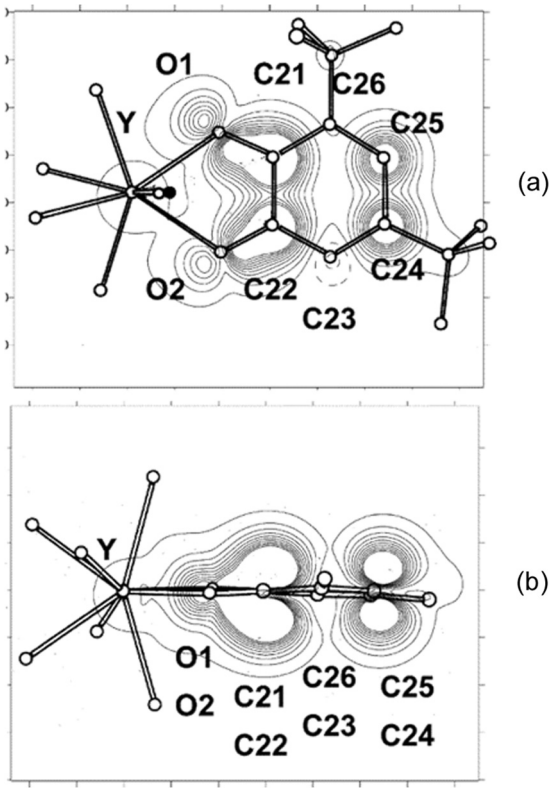

Figure 20. Projection of the induced spin density at 1.9 K under 9.5 T in $Y(HBPz_3)_2(DTBSQ)$ obtained by multipole model A reconstruction: (a) along the perpendicular to the mean plane of the semiquinonate ring; (b) along the C21-C22 direction. Reprinted with permission from Claiser, N., et al. 2005. *J. Phys. Chem. B* 109:2723–2732. Copyright 2005, American Chemical Society.[67]

attributed to antiferromagnetic coupling between the Y^{3+} ion and the DTBSQ radical anion. The polarized neutron data were taken at 1.9 K under an applied field of 9.5 T at the ILL. Figure 20 shows the spin density as reconstructed by multipolar refinement based on the polarized neutron diffraction data. The spin density from the anion is partially delocalized over the Y^{3+} site, which is primarily 5*s* in character and has virtually no 4*d* character (within error). This delocalization from the radical anion onto Y is most likely due to significant σ character on the oxygen atoms of the radical anion. This is consistent with results determined from

the experimental charge density obtained from the X-ray experiment, which revealed highly polarized oxygen atom lone pairs that carry a large negative charge on the semiquinone radical. Spin density on the carbon atoms of the ring is π-type in nature, which overlaps with the empty valence orbitals on Y, supporting the conclusion that the magnetic interaction between the rare earth ion and radical anion results from overlap of the magnetic orbitals of these two components of the complex.

Tutton salts of the first row transition metals, with formulas $A_2[M(H_2O)_6]X_2$ (A = alkali metal or ammonium, M = transition metal, X = sulfate or selenate), have been extensively studied by single crystal and powder diffraction (*vide ante*), and by polarized neutron diffraction (PND). Figgis and coworkers have investigated the spin density delocalization in the ammonium sulfate series of salts with transition metals V, Cr, Mn, Fe, and Ni using the ratio of the Bragg intensities from ''spin-up'' and ''spin-down'' polarized neutron diffraction. From these studies, the occupancies of the metal orbitals can be derived and spin density out to the hydrogen atoms on the water ligands were observed.[68]

Molecular magnets like the TCNE radical anion mentioned above are a popular research topic as of late. Polarized neutron diffraction will continue to be a very powerful tool in the complete characterization of these materials. During 2005, approximately 20% of all neutron scattering experiments at the ILL concerned magnetic materials;[69] over the 1994–2005 period a majority (55%) of single crystal scattering experiments concerned magnetism. This area of single crystal neutron scattering is poised to see a dramatic increase in interest as more advanced technologies become available.

NEUTRONS PRODUCE DATA FREE OF THE INFLUENCE OF ELECTRONIC EFFECTS

Because neutrons are diffracted from nuclei and generally do not interact with electrons, except in the case of magnetic materials, single crystal neutron diffraction data become valuable in electron charge density studies. The neutron data can accurately determine the atomic position and anisotropic ADPs of hydrogen atoms, information which is not available even from high resolution X-ray data. When X-ray and neutron diffraction data are collected at the same temperature, the hydrogen positions and anisotropic ADPs can be properly scaled and subsequently fixed during the multipole refinement of the charge density

from the X-ray data. The application of this procedure can be seen, for example, in the experimental electron density study of the peroxo complex $MoO(O_2)(HMPA)(dipic)$.[70] With neutron data determining the nuclear positions of atoms, bonding electron density can be accurately described using the X-ray data. The use of neutron parameters for hydrogen atoms in multipolar refinement of the experimental electron density has seen far more utilization in the study of small organic compounds, but with the availability of low temperature data from synchrotron sources and anticipated smaller crystal sizes for neutron diffraction, hopefully we will see an increase in the number of inorganic and organometallic complexes being studied.

A NOTE ON POWDER DIFFRACTION

Neutron powder diffraction has been used extensively over many years by materials scientists, physicists, and chemists alike. Every major neutron scattering center has one or more beamlines dedicated to powder diffraction. Sample volumes tend to be even larger than for single crystal diffraction; powder studies often require gram quantities of sample. Powder diffraction is thus problematic for materials containing highly absorbing elements; the large volume of sample will be absorbing and very little scattering will be observed. In this case, substitution to remove the highly absorbing isotope is the only way to get around the problem. Furthermore, powder diffraction is limited by unit cell size and by hydrogen-containing materials (*vide infra*).

Powder studies are sensitive to impurities in the sample; therefore, sample purity and size can be a challenging part of the experiment. Neutron powder diffraction has been invaluable in the investigation of oxide materials, where characterization with X-rays can be difficult due to the relatively low scattering power of oxygen compared to that of transition metals or heavier main group elements. The sensitivity to impurities can also be useful in those experiments following a chemical reaction over time, where products from complex reactions may be identified. Questions concerning site occupancy have also been a staple in powder diffraction experiments with neutrons.

Samples for powder neutron diffraction containing hydrogen are typically deuterated due to the high incoherent scattering of the hydrogen atom. In single crystal diffraction, deuteration is generally not required because the entire sample contributes both to coherent (Bragg scattering)

and incoherent scattering. In the powder experiment, the random orientation of many small crystallites creates the problem in which the entire sample in the neutron beam is contributing to incoherent scattering, but only a small portion of the sample is contributing to the coherent scatting. This results in a very high background for hydrogenated materials. By substituting deuterium for hydrogen, the scattering power of the sample increases (the scattering length of deuterium is approximately twice that for hydrogen, in absolute value) and the incoherent scattering is greatly reduced. For organometallic chemists, unfortunately the cost of perdeuterating a sample often will outweigh the benefit of pursuing neutron powder diffraction, in which case the only reasonable option is to attempt to grow a large single crystal.

THE FUTURE

What then does the future of single crystal neutron diffraction hold for us? Many of the challenges that we face in neutron crystallography of inorganic and organometallic compounds are currently being addressed. With the design of more intense neutron sources and new instrumentation optimized to handle the larger unit cells and complex structures that are becoming far more common in "small molecule" characterization, many of the barriers that in the past have limited the application of neutron diffraction are being removed.

A general purpose single crystal diffractometer, TOPAZ (see Figure 21), is currently under construction at the SNS and is scheduled for completion in early 2009 with user operations to commence later in 2009. The instrument design is optimized to handle sample sizes approaching that typically found for X-ray diffraction, approaching 0.1 mm^3 in volume or 0.5 mm on an edge. Measurements on materials with lattice parameters of 50 Å should be routine, thus expanding greatly on what we can currently address at existing sources. Plans for the instrument include a large number of detectors which, coupled with the increased flux on the sample, has the potential to decrease data collection times from several days or weeks to one day or perhaps even a few hours, depending on the sample.

A real strength of the TOPAZ instrument in small molecule crystallography, aside from the ability to collect data on smaller crystals and larger unit cell volumes, will likely be in parametric studies. Rapid data collection times will enable studies at variable temperature and/or

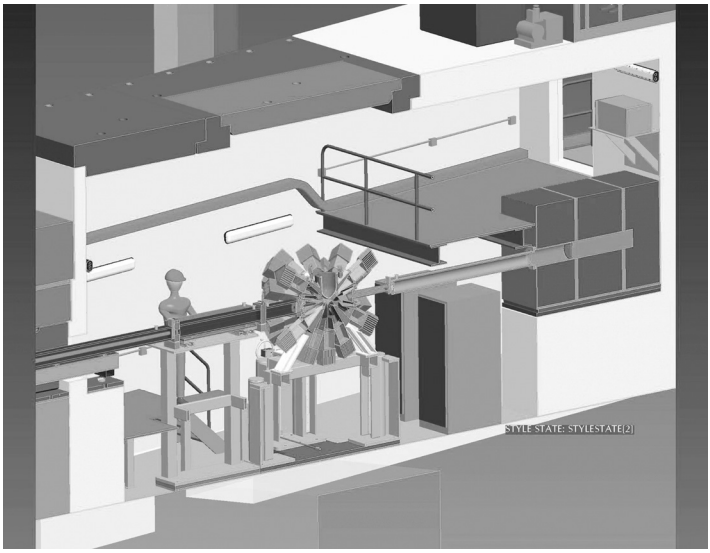

Figure 21. A cutaway diagram of the TOPAZ single crystal diffractometer currently under construction at the SNS. This instrument will be ideal for smaller sample sizes and larger unit cells, both of which currently limit the number of currently feasible problems in single crystal neutron diffraction. Figure courtesy of Christina Hoffmann, SNS, ORNL. For more information on the TOPAZ instrument, visit http://neutrons.ornl.gov/instrument_systems/beamline_12_topaz/index.shtml.

pressure, or systematic studies of a series of related compounds to compare features in the manner that we have outlined here above while discussing the structures from the Girolami group (see Figure 10). Problems involving hydrogen or other gas storage issues should also be relatively straightforward. More complex materials utilizing hydrogen bonding as a means of self-assembly, which often crystallize with large unit cell parameters, may be better understood with complete characterization by neutrons. Given the importance of hydrogen bonding in biological systems, bioinorganic chemistry problems are particularly well suited for study with an instrument such as TOPAZ due to the small size of crystals that typically can be grown.

TOPAZ may enable researchers to use the same small crystal for both X-ray and neutron studies, which would eliminate systematic sources of error in charge density studies. Plans for a flexible sample environment that include a magnet and polarizer for polarized neutron studies should enable users to engage in magnetic characterization of

materials, if not as a "day-one" capability on TOPAZ, then sometime in the near future. Tests of a compact ^{3}He polarizer and spin flipper at the IPNS over the last three years are important steps in achieving this capability.[71,72]

CONCLUSIONS

In this article we have outlined some of the major cases for utilizing single crystal neutron diffraction in research concerning inorganic and organometallic chemistry. In upcoming years, with advances being made in neutron source brightness and new instrumentation, access to single crystal neutron diffraction should become easier to obtain. The capability to handle smaller sample sizes will dramatically increase the number of problems we are able to examine. All of this is good news, especially for those researchers who in the past may have been unable to grow crystals of suitable size for neutron diffraction. Faster data collection times will enable researchers to perform parametric studies similar to those being done with X-ray diffraction, perhaps over a wider temperature range than can be performed at a laboratory X-ray source, as well as systematic studies of series of compounds exhibiting subtle changes due to sterics or electronics.

Getting started in neutron diffraction is as simple as contacting your friendly neighborhood instrument scientist and writing a proposal for beam time. Facility websites are the first place to look for contact information, details about instrument and sample environments, and proposal submission guidelines. Questions concerning the feasibility of an experiment can be addressed directly to the instrument scientist, and as a group we are always happy to answer questions!

ACKNOWLEDGEMENT

Work at Argonne National Laboratory was supported by the U.S. Department of Energy, Office of Science, Office of Basic Energy Sciences, under contract DE-AC02-06CH11357.

REFERENCES

1. Kealy, T. J. and P. L. Pauson, 1951. *Nature*, **168**, 1039–1040.
2. Wilkinson, G., M. Rosenblum, M. Whiting, and R. B. Woodward, 1952. *J. Am. Chem. Soc.*, **74**, 2125–2126.

3. Fischer, E. O. and W. Pfab, 1952. *Z. Naturforsch., B: Chem. Sci.*, **7**, 377–379.
4. Trofimenko, S. 1968. *J. Am. Chem. Soc.*, **90**, 4754.
5. Trofimenko, S. 1970. *Inorg. Chem.*, **9**, 2493.
6. Kosky, C. A., P. Ganis, and G. Avitabile, 1971. *Acta Cryst. B*, **27**, 1859.
7. Cotton, F. A., T. LaCour, and A. G. Stanislowski, 1974. *J. Am. Chem. Soc.*, **96**, 754.
8. Sheldrick, G. M. 1997. *SHELXL-97—A Program for Crystal Structure Refinement*, University of Goettingen, Germany.
9. Larson, A. C. and R. B. Von Dreele, 2000. *General Structure Analysis System—GSAS*. Los Alamos National Laboratory.
10. Wilson, C. C. 2000. *Single Crystal Neutron Diffraction From Molecular Materials*, World Scientific Publishing Co. Pte. Ltd, Singapore.
11. Wilson, C. C. 2005. *Z. Kristallogr.* **220**, 385–398.
12. Koetzle, T. F. and A. J. Schultz, 2005. *Top. Catal.*, **32**, 251–255.
13. Pynn, R. 1990. *Los Alamos Science*, **19**, 1–31.
14. Calvert, R. B., J. R. Shapley, A. J. Schultz, J. M. Williams, S. L. Suib, and G. D. Stucky, 1978. *J. Am. Chem. Soc.*, **100**, 6240.
15. Bau, R., M. H. Drabnis, L. Garlaschelli, W. T. Klooster, Z. Xie, T. F. Koetzle, and S. Martinengo, 1997. *Science*, **275**, 1099.
16. Spencer, E. C., J. A. K. Howard, G. J. McIntyre, J. L. C. Rowsell, and O. M. Yaghi, 2006. *Chem. Commun.*, 278–280.
17. Anderson, T. M., W. A. Neiwert, M. L. Kirk, P. M. B. Piccoli, A. J. Schultz, T. F. Koetzle, D. G. Musaev, K. Morokuma, R. Cao, and C. L. Hill, 2004. *Science*, **306**, 2074–2077.
18. Tippe, A. and W. C. Hamilton, 1969. *Inorg. Chem.*, **8**, 464–470.
19. http://www.ncnr.nist.gov/resources/n-lengths/ As taken from: 1992. *Neutron News*, **3**, 29–37.
20. Allen, F. H. 2002. *Acta. Cryst. B*, **58**, 380–388.
21. Teller, R. G. and R. Bau, 1981. *Struct. Bonding*, **44**, 1.
22. Bau, R. and M. H. Drabnis, 1997. *Inorg, Chim. Acta*, **259**, 27–50.
23. Yousufuddin, M., J. Baldamus, O. Tardif, Z. Hou, S. A. Mason, G. J. McIntyre, and R. Bau, 2006. *Physica B*, **385–386**, 231–233.
24. Boss, S. R., J. M. Cole, R. Haigh, R. Snaith, A. E. H. Wheatley, G. J. McIntyre, and P. R. Raithby, 2004. *Organometallics*, **23**, 4527.
25. Webster, C. E., C. L. Gross, D. M. Young, G. S. Girolami, A. J. Schultz, M. B. Hall, and J. Eckert, 2005. *J. Am. Chem. Soc.*, **127**, 15091–15101.
26. Kubas, G. 2001. *Metal Dihydrogen and Sigma-Bond Complexes: Structure, Theory, and Reactivity*, Kluwer Academic/Plenum Publishers, New York.
27. Li, H., M. Eddaoudi, M. O'Keeffe, and O. M. Yaghi, 1999. *Nature*, **402**, 276.
28. Rowsell, J. L. C., J. Eckert, and O. M. Yaghi, 2005. *J. Am. Chem. Soc.*, **127**, 14904–14910.
29. Brookhart, M. and M. L. H. Green, 1983. *J. Organomet. Chem.*, **250**, 395.

30. Crabtree, R. H. 1993. *Angew. Chem. Int. Ed. Engl.*, **32**, 789.
31. Collman, J. P., L. S. Hegedus, J. R. Norton, and R. G. Finke, 1987. *Principles and Applications of Organotransition Metal Chemistry*, University Science Books, Mill Valley, CA.
32. Elschenbroich, C. and A. Salzer, 1992. *Organometallics: A Concise Introduction*, VCH Publishers Inc., New York.
33. Cosky, C. A., P. Ganis, and G. Avitabile, 1971. *Acta Cryst.*, **B27**, 1859.
34. Piccoli, P. M. B., J. A. Cowan, A. J. Schultz, T. F. Koetzle, and S. Trofimenko, 2005. *Am. Crystallographic Assoc. Meeting Abstracts*, Orlando, FL.
35. Dawoodi, Z., M. L. H. Green, V. S. B. Mtetwa, K. Prout, A. J. Schultz, J. M. Williams, and T. F. Koetzle, 1986. *J. Chem. Soc. Dalton Trans.*, 1629.
36. Dawoodi, Z., M. L. H. Green, V. S. B. Mtetwa, and K. Prout, 1982. *J. Chem. Soc., Chem. Commun.*, 1410.
37. Bau, R., S. A. Mason, B. O. Patrick, C. S. Adams, W. B. Sharp, and P. Legzdins, 2001. *Organometallics*, **20**, 4492–4501.
38. Debad, J. D., P. Legzdins, S. J. Rettig, and J. E. Veltheer, 1993. *Organometallics*, **12**, 2714.
39. Baratta, W., C. Mealli, E. Herdtweck, A. Ienco, S. A. Mason, and P. Rigo, 2004. *J. Am. Chem. Soc.*, **126**, 5549–5562.
40. Mork, B. V., T. D. Tilley, A. J. Schultz, and J. A. Cowan, 2004. *J. Am. Chem. Soc.*, **126**, 10428–10440.
41. Mork, B. V. and T. D. Tilley, 2003. *Angew. Chem. Int. Ed. Engl.*, **42**, 357–360.
42. Scherer, W. and G. S. McGrady, 2004. *Angew. Chem. Int. Ed.*, **43**, 1782–1806.
43. Peterson, S. W. and H. A. Levy, 1952. *J. Chem. Phys.*, **20**, 704–707.
44. Steiner, T. 1998. *J. Phys. Chem. A*, **102**, 7041–7052.
45. Schoenborn, B. P. and R. B. Knott, 1997. *Neutrons in Biology*, Plenum Publishing Corporation, New York.
46. Langan, P., G. Greene, and B. P. Schoenborn, 2004. *J. Appl. Cryst.*, **37**, 24–31.
47. Schultz, A. J., P. Thiyagarajan, J. P. Hodges, C. Rehm, D. A. A. Myles, P. Langan, and A. D. Mesecar, 2005. *J. Appl. Cryst.*, **38**, 964–974.
48. Brammer, L., J. R. Helliwell, C. C. Wilson, D. A. Keen, and P. G. Radaelli, 2005. LMX – A Diffractometer for Large Molecule Crystallography. Located at http://www.isis.rl.ac.uk/targetstation2/instruments/phase2/lmx2005Web.pdf
49. Cotton, F. A., C. K. Fair, G. E. Lewis, G. N. Mott, F. K. Ross, A. J. Schultz, and J. M. Williams, 1984. *J. Am. Chem. Soc.*, **106**, 5319–5323.
50. Hathaway, B. J. and A. W. Hewat, 1984. *J. Solid State Chem.*, **51**, 364–375.
51. Simmons, C. J., M. A. Hitchman, H. Stratemeier, and A. J. Schultz, 1993. *J. Am. Chem. Soc.*, **115**, 11304–11311.
52. Schultz, A. J., R. Henning, M. A. Hitchman, and H. Stratemeier, 2003. *Crystal Growth & Design*, **3**, 403–407.

53. Henning, R., A. J. Schultz, M. A. Hitchman, G. Kelly, and T. Astley, 2000. *Inorg. Chem.*, **39**, 765–769.
54. Desiraju, G. R. 2002. *Acc. Chem. Res.*, **35**, 565–573.
55. Braga, D. and F. Grepioni, 2000. *Acc. Chem. Res.*, **33**, 601–608.
56. Brammer, L., E. A. Bruton, and P. Sherwood, 2001. *Crystal Growth & Design*, **1**, 227–290.
57. Vicic, D. A., T. J. Anderson, J. A. Cowan, and A. J. Schultz, 2004. *J. Am. Chem. Soc.*, **126**, 8132–8133.
58. Tyree, W. S., D. A. Vicic, P. M. B. Piccoli, and A. J. Schultz, 2006. *Inorg. Chem.*, **45**, 8853–8855.
59. Kriley, C. E., C. J. Woolley, M. K. Krepps, E. M. Popa, P. E. Fanwick, and I. P. Rothwell, 2000. *Inorg. Chim. Acta*, **300–302**, 200–205.
60. Sieve, B., X. Z. Chen, R. Henning, P. Brazis, C. R. Kannewurf, J. A. Cowen, A. J. Schultz, and M. G. Kanatzidis, 2001. *J. Am. Chem. Soc.*, **123**, 7040–7047.
61. Zhuravleva, M. A., X. Wang, A. J. Schultz, T. B. Bakas, and M. G. Kanatzidis, 2002. *Inorg. Chem.*, **41**, 6056–6061.
62. Condron, C. L., J. Martin, G. S. Nolas, P. M. B. Piccoli, A. J. Schultz, and S. M. Kauzlarich, 2006. *Inorg. Chem.*, **45**, 9381–9386.
63. Bullock, R. M., L. Brammer, A. J. Schultz, A. Albinati, and T. F. Koetzle, 1992. *J. Am. Chem. Soc.*, **114**, 5125–5130.
64. Brammer, L., J. A. K. Howard, O. Johnson, T. F. Koetzle, J. L. Spencer, and A. M. Stringer, 1991. *J. Chem. Soc. Chem. Commun.*, 241–243.
65. Albinati, A., R. M. Bullock, B. J. Rappoli, and T. Koetzle, 1991. *Inorg. Chem.*, **30**, 1414–1417.
66. Zheludev, A., A. Grand, E. Ressouche, J. Schweizer, B. G. Morin, A. J. Epstein, D. A. Dixon, and J. S. Miller, 1994. *J. Am. Chem. Soc.*, **116**, 7243–7249.
67. Claiser, N., M. Souhassou, C. Lecomte, B. Gillon, C. Carbonera, A. Caneschi, A. Dei, D. Gatteschi, A. Bencini, Y. Pontillon, and E. Leliévre-Berna, 2005. *J. Phys. Chem. B*, **109**, 2723–2732.
68. Chandler, G. S., G. A. Christos, B. N. Figgis, and P. A. Reynolds, 1992. *J. Chem. Soc. Faraday Trans.*, **88**, 1961–1969.
69. 2005. ILL Annual Report 2005.
70. Macchi, P., A. J. Schultz, F. K. Larsen, and B. B. Iversen, 2001. *J. Phys. Chem. A*, **105**, 9231–9242.
71. Jones, G. L., J. Bakera, W. C. Chen, B. Colletta, J. A. Cowan, M. F. Dias, T. R. Gentile, C. Hoffmann, T. Koetzle, W. T. Lee, K. Littrell, M. Miller, A. Schultz, W. M. Snow, X. Tong, H. Yan, and A. Yue, 2005. *Physica B*, **356**, 86–90.
72. Jones, G. L., F. Dias, B. Collett, W. C. Chen, T. Gentile, P. M. B. Piccoli, M. E. Miller, A. J. Schultz, H. Y. Yan, X. Tong, M. Snow, W. T. Lee, C. Hoffmann, and J. Thomison, 2006. *Physica B*, **385–386**, 1131–1133.